

Calculation of Solvation Free Energy Using RISM Theory for Peptide in Salt Solution

MASAHIRO KINOSHITA,¹ YUKO OKAMOTO,² FUMIO HIRATA²

¹Advanced Energy Utilization Division, Institute of Advanced Energy, Kyoto University, Uji, Kyoto 611, Japan

²Department of Theoretical Studies, Institute for Molecular Science, Okazaki, Aichi 444, Japan

Received 30 June 1997; accepted 2 July 1998

ABSTRACT: We developed a robust, highly efficient algorithm for solving the full reference interaction site model (RISM) equations for salt solutions near a solute molecule with many atomic sites. It was obtained as an extension of our previously reported algorithm for pure water near the solute molecule. The algorithm is a judicious hybrid of the Newton–Raphson and Picard methods. The most striking advantage is that the Jacobian matrix is just part of the input data and need not be recalculated at all. To illustrate the algorithm, we solved the full RISM equations for a dipeptide ($\text{NH}_2\text{—CHCH}_3\text{—CONH—CHCH}_3\text{—COOH}$) in a 1 M NaCl solution. The extended simple point charge (SPC/E) model was employed for water molecules. Two different conformations of the dipeptide were considered. It was assumed for each conformation that the dipeptide was present either as an un-ionized form or as a zwitterion. The structure of the salt solution near the dipeptide and salt effects on the solvation free energy were also discussed. © 1998 John Wiley & Sons, Inc. *J Comput Chem* 19: 1724–1735, 1998

Keywords: reference interaction site model (RISM) theory; salt solution; peptide; protein; solvation free energy

Correspondence to: M. Kinoshita; e-mail: kinoshit@iae.kyoto-u.ac.jp

Contract/grant sponsor: Joint Studies Program of the Institute for Molecular Science; Japanese Ministry of Education, Science, Sports, and Culture

Introduction

A full theory of the conformations of biopolymers requires a method for treating the effects of a solvent on the induced structures. The reference interaction site model (RISM) theory provides this type of method, and there is no comparable theoretical alternative that potentially allows us to analyze the stability of a biopolymer-solvent system on an atomic level. Our ultimate goal was to develop an algorithm for solving the full RISM equations for a biopolymer-salt solution system without a huge amount of computation load.

In our previous article¹ we reported a robust and extremely efficient algorithm for solving the RISM equations for pure water (the extended simple point charge, SPC/E, model water²) near a solute molecule with many atomic sites (interaction sites) such as peptides. The water structure near a peptide and its solvation free energy were calculated without using the superposition approximation^{3,4} in which the entire free energy of the peptide is expressed as a sum of the potential of mean forces between pairs of atoms. The most important feature of the algorithms is that the Jacobian matrix is just part of the input data and need not be recalculated at all.

We once compared our algorithm with the conventional Picard method for Acrolein (a solute molecule with eight atomic sites) in pure water and found that the results from the two calculations were the same, but our algorithm was over 100 times faster. We tried to make another comparison for Met-enkephalin (a peptide with 75 atomic sites) in pure water, but we could never obtain a converged result with the Picard method despite our efforts in setting the initial guesses and changing the mixing parameters to extremely small values. In contrast, with our algorithm it was quite easy to achieve convergence.¹ For a solute molecule in salt solutions with finite salt concentrations, matters get more serious when the Picard method is employed.⁵

In this article we extend our previous algorithm to salt solutions near a peptide. The algorithm is demonstrated for a dipeptide with 23 atomic sites ($\text{NH}_2\text{—CHCH}_3\text{—CONH—CHCH}_3\text{—COOH}$; Ala-Ala) in a 1 M NaCl solution. It is shown that the robustness and high efficiency of the algorithm is not deteriorated by the inclusion of ions in water, in contrast with the general experience⁵ that an

algorithm becomes quite unstable once ions are included. Two different conformations of the dipeptide are considered in three different cases. In cases 1 and 2 the dipeptide is un-ionized, but in case 3 it is present as a zwitterion ($\text{NH}_3^+\text{—CHCH}_3\text{—CONH—CHCH}_3\text{—COO}^-$). In case 1 all the site charges of the dipeptide are set to zero (i.e., the dipeptide in case 1 is completely hydrophobic), but in cases 2 and 3 the full values are assigned to the site charges. In earlier articles we analyzed the salt effects on the solubility of noble gases in water⁶ and the structure of pure water near a peptide and the corresponding solvation free energy.⁷ As an extension of these analyses, in this article we discuss the structure of the 1 M NaCl solution near the dipeptide and salt effects on the solvation free energy.

Perkyns and colleagues^{8,9} solved the full RISM equations for a model of a zwitterionic tripeptide (Gly-Ala-Gly) in high concentration NaCl solution. The Picard method was employed in their work. Their results conflicts with ours in the following two respects: they claim that there are no solutions of the RISM theory for the system below 3 M, and the peptide is salted into solution by NaCl. We emphasize the following: we thoroughly verified that true convergence is attained in our calculations. Although the reasons for the conflict must be clarified in further studies, it is possible that even qualitative aspects of the behavior of a peptide-salt solution system is strongly dependent on the peptide species.

Theory

The subscripts *V*, *C*, *A*, *E*, and *S* denote water, cation, anion, electrolyte solution (salt solution), and solute molecule, respectively. It is assumed that the solute molecules are present at infinite dilution. The calculation process is then split into two steps where the bulk salt solution (step 1) and the salt solution near a solute molecule (step 2) are treated. The site-site intermolecular total correlation functions calculated in step 1 are used as input variables for step 2. The calculation in step 1 is performed using the RISM theory improved by Perkyns and Pettitt^{10,11} that assures the dielectric consistency and realistic structural and thermodynamic properties: the dielectric constant determined in real experiments is read as part of the input data⁶ and the long-range structure is improved so that the dielectric constant equals the input value. We consider step 2 hereafter.

It is assumed that the solute molecule, a water molecule, a cation, and an anion have m , 3, 1, and 1 interaction sites, respectively. The site-site Ornstein-Zernike (SSOZ) equation is expressed as

$$\tilde{\eta}_{SE} = \tilde{\mathbf{w}}_{SS} \tilde{\mathbf{c}}_{SE} \tilde{\mathbf{H}}_{EE} - \tilde{\mathbf{c}}_{SE}, \quad (1a)$$

$$\tilde{\eta}_{SE} = \tilde{\mathbf{h}}_{SE} - \tilde{\mathbf{c}}_{SE}, \quad (1b)$$

$$\tilde{\mathbf{H}}_{EE} = \tilde{\mathbf{w}}_{EE} + \boldsymbol{\rho}_E \tilde{\mathbf{h}}_{EE}, \quad (2)$$

where $\tilde{\mathbf{H}}_{EE}$, $\tilde{\eta}_{SE}$, and $\tilde{\mathbf{w}}_{SS}$ are 5×5 , $m \times 5$, and $m \times m$ matrices, respectively; $\boldsymbol{\rho}_E$ is the matrix of the number density of water molecules, cations, and anions in the bulk; \mathbf{h} is the matrix of site-site intermolecular total correlation functions; \mathbf{c} is the matrix of site-site intermolecular direct correlation functions; \mathbf{w} is the intramolecular correlation matrix; and the tilde (\sim) represents Fourier transforms. The $\tilde{\mathbf{H}}_{EE}$ depends on the properties of the bulk salt solution alone and is part of the input data for step 2. The $\tilde{\mathbf{w}}_{SS}$, $\tilde{\mathbf{w}}_{EE}$, $\boldsymbol{\rho}_E$, \mathbf{h}_{EE} , and $\tilde{\mathbf{H}}_{EE}$ are symmetrical matrices. The expressions of some of the matrices are

$$\boldsymbol{\rho}_E = \begin{pmatrix} \rho_V & 0 & 0 & 0 & 0 \\ 0 & \rho_V & 0 & 0 & 0 \\ 0 & 0 & \rho_V & 0 & 0 \\ 0 & 0 & 0 & \rho_C & 0 \\ 0 & 0 & 0 & 0 & \rho_A \end{pmatrix} \quad (3)$$

$$\tilde{\mathbf{c}}_{SE} = \begin{pmatrix} \tilde{c}_{1H} & \tilde{c}_{1O} & \tilde{c}_{1H} & \tilde{c}_{1C} & \tilde{c}_{1A} \\ \vdots & \vdots & \vdots & \vdots & \vdots \\ \tilde{c}_{mH} & \tilde{c}_{mO} & \tilde{c}_{mH} & \tilde{c}_{mC} & \tilde{c}_{mA} \end{pmatrix} \quad (4)$$

$$\tilde{\mathbf{w}}_{SS} = \begin{pmatrix} 1 & \tilde{w}_{12} & \cdots & \tilde{w}_{1m} \\ \tilde{w}_{21} & 1 & \cdots & \tilde{w}_{2m} \\ \vdots & \vdots & \ddots & \vdots \\ \tilde{w}_{m1} & \tilde{w}_{m2} & \cdots & 1 \end{pmatrix} \quad (5a)$$

and

$$\tilde{w}_{aa'} = \tilde{w}_{a'a} = \sin(kl_{aa'})/(kl_{aa'}), \quad (5b)$$

where k is the wave number and $l_{aa'}$ is the distance between sites a and a' in the solute molecule.

The closure equation employed is of the hypernetted-chain (HNC) type given by

$$\begin{aligned} c_{ab}(r) &= \exp\{-u_{ab}(r)/(k_B T) + \eta_{ab}(r)\} \\ &\quad - \eta_{ab}(r) - 1, \\ a &= 1, \dots, m; b = H, O, C, A; \end{aligned} \quad (6)$$

where u_{ab} is the pair potential between sites a and b ; and k_B is the Boltzmann constant; and a and b denote sites in the solute molecule and in the salt solution, respectively.

The solvation free energy for the solute molecule $\Delta\mu_S$ is calculated from^{6,7,12,13}

$$\Delta\mu_S/(k_B T) = 4\pi \int_0^\infty r^2 F(r) dr, \quad (7a)$$

$$\begin{aligned} F(r) &= \sum_{a=1}^m \sum_{b=H,O,C,A} \rho_b [\{h_{ab}(r)\}^2/2 \\ &\quad - c_{ab}(r) - h_{ab}(r)c_{ab}(r)/2], \quad (7b) \end{aligned}$$

$$\rho_H = 2\rho_V, \quad \rho_O = \rho_V, \quad \rho_C = \rho_A. \quad (7c)$$

The site-site correlation functions $h_{ab}(r)$ and $c_{ab}(r)$ are calculated by solving eqs. (1) and (6). It is convenient to decompose $\Delta\mu_S$ into I_V , I_C , and I_A ($\Delta\mu_S = I_V + I_C + I_A$). I_V , I_C , and I_A are interdependent but can be regarded as contributions of structures of water molecules ($b = H, O$), cations ($b = C$), and anions ($b = A$) near the solute molecule, respectively.⁶ The solvation free energy for the solute molecule in pure water is denoted by $\Delta\mu_{S0}$: $\Delta\mu_{S0} = I_V$ in the pure water case.

Algorithm

A sufficiently long range r_L is divided into N mesh points ($r_i = i \delta r$, $i = 0, 1, \dots, N-1$; $\delta r = r_L/N$) and all the functions are represented by their values on these points. We have found that here r_L must be longer than that in the pure water case. In the present analysis, δr and N are set at $0.02d$ ($d = 0.28$ nm) and 1024, respectively. We iterate on $\eta_{ab}(r_i)$ (there are $4m$ distinct pairs). $\eta_{ab}(r_i)$ for $r_i \leq D$ ($D \ll r_L$) are decomposed into "coarse" and "fine" variables using the projective representation described in our previous articles.^{14,15} $\eta_{ab}(r_i)$ for $r_i > D$ are treated as fine variables. The coarse and fine variables are converged in the inner Newton-Raphson and outer Picard loops, respectively. The values of i_{Bt} and κ_t ($t = 1, \dots, 4m$; $2i_{Bt} \delta r$ and κ_t denote the width and the number of the roof basis functions, respectively) can all be different.¹⁴ The dimensionality of the Jacobian matrix can be greatly reduced by choosing a large value for i_{Bt} . D is chosen such that $\exp\{-u_{ab}(r_i)/(k_B T) + \eta_{ab}(r_i)\}$ is sufficiently smaller than 1 for $r_i \leq D$. As a result, the Jacobian matrix becomes almost independent of the solute molecule-water and

-ion correlations. The matrix can then be treated as part of the input data^{1, 14, 15}: it is constant against changes in the iteration variables. Even the same matrix can be used for a set of different conformations of the solute molecule.¹

As given by eq. (4), the first and third columns of $\tilde{\mathbf{c}}_{\text{SE}}$ are identical, and this is also true for $\tilde{\mathbf{\eta}}_{\text{SE}}$. Using this feature of the matrices, we rewrite the SSOZ equation as follows so that it can be handled most efficiently:

$$(\tilde{\mathbf{\eta}}_{\text{SE}})_{ij} = (\tilde{\mathbf{w}}_{\text{SS}}\tilde{\mathbf{c}}_{\text{SE}}\tilde{\mathbf{H}}_{\text{EE}})_{ij} - (\tilde{\mathbf{c}}_{\text{SE}})_{ij}, \quad (8)$$

$$(\tilde{\mathbf{c}}_{\text{SE}}\tilde{\mathbf{H}}_{\text{EE}})_{nj} = \xi_{\text{H}}(j)(\tilde{\mathbf{c}}_{\text{SE}})_{n1} + \xi_{\text{O}}(j)(\tilde{\mathbf{c}}_{\text{SE}})_{n2} + \xi_{\text{C}}(j)(\tilde{\mathbf{c}}_{\text{SE}})_{n3} + \xi_{\text{A}}(j)(\tilde{\mathbf{c}}_{\text{SE}})_{n4}, \\ n = 1, \dots, m; \quad j = 1, 2, 3, 4; \quad (9)$$

$$(\tilde{\mathbf{w}}_{\text{SS}}\tilde{\mathbf{c}}_{\text{SE}}\tilde{\mathbf{H}}_{\text{EE}})_{ij} = \sum_{n=1}^m (\tilde{\mathbf{w}}_{\text{SS}})_{in}(\tilde{\mathbf{c}}_{\text{SE}}\tilde{\mathbf{H}}_{\text{EE}})_{nj}, \\ i = 1, \dots, m; \quad j = 1, 2, 3, 4; \quad (10)$$

$$\xi_{\text{H}}(j) = (\tilde{\mathbf{H}}_{\text{EE}})_{1j} + (\tilde{\mathbf{H}}_{\text{EE}})_{3j} \quad \text{for } j = 1, 2; \quad (11a)$$

$$\xi_{\text{H}}(j) = 2(\tilde{\mathbf{H}}_{\text{EE}})_{1j_1}, \quad j_1 = j + 1 \quad \text{for } j = 3, 4; \quad (11b)$$

$$\xi_{\text{O}}(j) = (\tilde{\mathbf{H}}_{\text{EE}})_{2j} \quad \text{for } j = 1, 2; \quad (11c)$$

$$\xi_{\text{O}}(j) = (\tilde{\mathbf{H}}_{\text{EE}})_{2j_1}, \quad j_1 = j + 1 \quad \text{for } j = 3, 4; \quad (11d)$$

$$\xi_{\text{C}}(j) = (\tilde{\mathbf{H}}_{\text{EE}})_{4j} \quad \text{for } j = 1, 2; \quad (11e)$$

$$\xi_{\text{C}}(j) = (\tilde{\mathbf{H}}_{\text{EE}})_{4j_1}, \quad j_1 = j + 1 \quad \text{for } j = 3, 4; \quad (11f)$$

$$\xi_{\text{A}}(j) = (\tilde{\mathbf{H}}_{\text{EE}})_{5j} \quad \text{for } j = 1, 2; \quad (11g)$$

$$\xi_{\text{A}}(j) = (\tilde{\mathbf{H}}_{\text{EE}})_{5j_1}, \quad j_1 = j + 1 \quad \text{for } j = 3, 4; \quad (11h)$$

where $(\mathbf{X})_{ij}$ represents the (i, j) element of the matrix \mathbf{X} , and $\xi_b(j)$ ($b = \text{H, O, C, and A}$) are read from a data file.

It can be shown from eqs. (8) to (11) that

$$\partial(\tilde{\mathbf{\eta}}_{\text{SE}})_{ij}/\partial(\tilde{\mathbf{c}}_{\text{SE}})_{n1} = \xi_{\text{H}}(j)(\tilde{\mathbf{w}}_{\text{SS}})_{in} - \delta_{in}\delta_{j1}, \\ i, n = 1, \dots, m; \quad j = 1, 2, 3, 4; \quad (12a)$$

$$\partial(\tilde{\mathbf{\eta}}_{\text{SE}})_{ij}/\partial(\tilde{\mathbf{c}}_{\text{SE}})_{n2} = \xi_{\text{O}}(j)(\tilde{\mathbf{w}}_{\text{SS}})_{in} - \delta_{in}\delta_{j2}, \quad (12b)$$

$$\partial(\tilde{\mathbf{\eta}}_{\text{SE}})_{ij}/\partial(\tilde{\mathbf{c}}_{\text{SE}})_{n3} = \xi_{\text{C}}(j)(\tilde{\mathbf{w}}_{\text{SS}})_{in} - \delta_{in}\delta_{j3}, \quad (12c)$$

$$\partial(\tilde{\mathbf{\eta}}_{\text{SE}})_{ij}/\partial(\tilde{\mathbf{c}}_{\text{SE}})_{n4} = \xi_{\text{A}}(j)(\tilde{\mathbf{w}}_{\text{SS}})_{in} - \delta_{in}\delta_{j4}, \quad (12d)$$

where δ denotes Kronecker's delta. As in the pure water case,¹ the right-hand sides of eq. (12) are completely independent of the solute molecule-water and -ion correlations. An analytical expression of the Jacobian matrix is then derived and arranged in a compact form so that the matrix can be constructed quite efficiently using the fast Fourier transform^{1, 14, 15} (FFT).

At each Newton-Raphson iterative step, the linear set of equations written as

$$\mathbf{J}\mathbf{x} = \mathbf{b} \quad (13)$$

must be solved for \mathbf{x} (\mathbf{J} is the Jacobian matrix, \mathbf{x} is the column vector, the components of which are unknown corrections of the independent variables, and \mathbf{b} is the column vector comprising known numbers). This is efficiently solved as described in our previous article.¹

The long-range Coulomb potentials are handled in a special manner without using the so-called renormalization technique so that the number of mesh points N can be minimized.¹

Because the Jacobian matrix is determined from the bulk properties and the intramolecular correlations of the solute molecule, it is completely independent of initial guesses of the iteration variables. Therefore, the calculation never becomes unstable even with crude initial guesses. This is in marked contrast with the usual Newton-Raphson method where the matrix can be pathological and give rise to severe instability unless the initial guesses are sufficiently good. We propose the simple setting expressed as

$$\eta_{ab}(r) = q_a q_b / (k_{\text{B}} T r) \quad \text{for } r \geq r_{ab}, \quad (14a)$$

$$\eta_{ab}(r) = q_a q_b / (k_{\text{B}} T r_{ab}) \quad \text{for } r \leq r_{ab}. \quad (14b)$$

In the above setting

$$r_{ab} \sim \kappa d \quad \text{for } q_a q_b > 0, \quad (15a)$$

$$r_{ab} \sim r_0 \quad \text{for } q_a q_b < 0, \quad (15b)$$

where $u_{ab}(r_0) \sim 0$ and $\kappa \sim 0.8$ for $b = \text{H}$ and $\kappa \sim 1.0$ for $b = \text{O, C, and A}$. The parameters, $i_{\text{B}t}$ and κ_t , are chosen such that $i_{\text{B}t}\kappa_t \delta r \sim r_{ab}$ ($i_{\text{B}t}$ is set

to 4). We found, however, that convergence properties improve significantly when $i_{\text{Bt}} \kappa_t \delta r$ are set to larger values for $b = \text{C}$ and A .

The calculation is considered converged once

$$E_{\text{out}} = \sum_{j=1}^{N_f} |(\gamma_j^{\text{new}} - \gamma_j^{\text{old}}) / \gamma_j^{\text{new}}| / N_f < 10^{-5} \quad (16)$$

is satisfied in the outer loop (γ_j denote the fine variables; N_f is the total number of the fine variables; and the superscripts new and old represent the new and old values, respectively). With this convergence criterion the solvation free energy can be calculated with the accuracy of ± 0.3 kcal/mol (0.6 kcal/mol $\sim k_B T$). We further consider E_p , defined by

$$E_p = \sum_{a=1}^m \sum_{b=\text{H}, \text{O}, \text{C}, \text{A}} \sum_{i=0}^{N-1} |\eta_{ab}(r_i)^{\text{new}} - \eta_{ab}(r_i)^{\text{old}}| / (4mN), \quad (17)$$

where $\eta_{ab}(r_i)^{\text{new}}$ are calculated from one cycle of the RISM-HNC theory; $c_{ab}(r_i)^{\text{old}}$ are calculated from $\eta_{ab}(r_i)^{\text{old}}$ using the HNC equation, $\tilde{c}_{ab}(k_j)^{\text{old}}$ ($k_j = j \delta k$, $j = 0, 1, \dots, N-1$; $\delta k = \pi/(\delta r N)$) are determined via the forward Fourier transformation; $\tilde{\eta}_{ab}(k_j)^{\text{new}}$ are calculated from $\tilde{c}_{ab}(k_j)^{\text{old}}$ using the SSOZ equation; and $\eta_{ab}(r_i)^{\text{new}}$ are obtained via the back Fourier transformation. It has been verified that the convergence criterion.

$$E_p < \varepsilon_p, \quad (18)$$

which is used in the usual Picard method, is always satisfied with $\varepsilon_p = 10^{-5}$. In the zwitterion case (case 3), criterion (18) with $\varepsilon_p = 10^{-12}$ was also tested. It was verified that the results obtained from criterion (16) and criterion (18) with $\varepsilon_p = 10^{-12}$ are indistinguishable and true convergence is attained with criterion (16). We note that $\varepsilon_p = 10^{-5}$ is sufficiently small but our value ($\varepsilon_p = 10^{-12}$) is even 7 orders of magnitude smaller than this. This thorough (but usually unnecessary) verification is necessitated for the following reason: Perkyns et al.^{8,9} reported that the RISM-HNC theory possessed no solutions for a zwitterionic tripeptide of sequence Gly-Ala-Gly in NaCl solution when the salt concentration was below 3 M, which clearly conflicts with our result; and we therefore need to give an assurance of true convergence of our calculations.

Model

A computer program was written in FORTRAN statements to demonstrate the robustness and high efficiency of the algorithm. The dipeptide previously studied⁷ was chosen for the demonstration. All the calculations were performed on a workstation at the Institute for Molecular Science (IBM RS6000/3CT, 64 MB). The potential energy functions and parameters employed for the dipeptide were those based on ECEPP/2.¹⁶⁻¹⁹ The model of a water molecule was the SPC/E model.² The temperature was set at 298.15 K. The $u_{ab}(r)$ has the form

$$u_{ab}(r) = q_a q_b / r + 4\varepsilon_{ab} \{ (\sigma_{ab}/r)^{12} - (\sigma_{ab}/r)^6 \}, \\ a = 1, \dots, m; \quad b = \text{H}, \text{O}, \text{C}, \text{A}; \quad (19)$$

and the standard combination rule

$$\varepsilon_{ab} = (\varepsilon_a \varepsilon_b)^{1/2}, \quad \sigma_{ab} = (\sigma_a + \sigma_b)/2 \quad (20)$$

is employed for calculating the Lennard-Jones potential parameters. The salt solution tested was a 1 M NaCl solution. The potential parameters used in the bulk calculation (step 1) were those of Pettitt and Rossky.²⁰ The dimensionless number densities, $\rho_V d^3$ and $\rho_C d^3$, and the dielectric constant for the bulk 1 M NaCl solution are given in ref. 6. The σ values for Na^+ and Cl^- in the calculation of step 2 are taken from those in the water-ion interactions in ref. 20: $\sigma_C = 0.226$ nm and $\sigma_A = 0.392$ nm. The ε values are calculated from Mavroyannis-Stephen theory²¹ ($\varepsilon_C = 0.293$ kcal/mol and $\varepsilon_A = 0.448$ kcal/mol).

As in our earlier work,⁷ two different conformations of the dipeptide are treated, and three different cases are considered for each conformation. In cases 1 and 2 the dipeptide is un-ionized, but in case 3 it is ionized and present as a zwitterion. In case 1 all the site charges of the dipeptide are set to zero, but in cases 2 and 3 the full values are assigned to the site charges. The two conformations in the un-ionized cases (cases 1 and 2) are shown in Figure 1. The conformational energies for conformations 1 and 2 in case 2 are 4.6 and 38.2 kcal/mol, respectively. Conformation 1 is the lowest energy conformation in the gas phase determined by Monte Carlo simulated annealing.⁷ A feature of conformation 2 is that the three oxygen atoms are close to one another and 11 O Ala¹ and 21 O Ala² are sufficiently far apart from the methyl

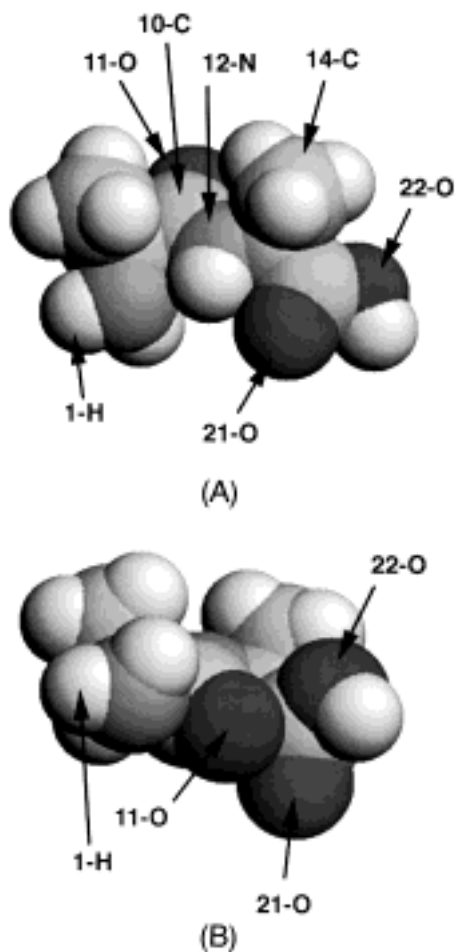


FIGURE 1. Conformations of the dipeptide considered (in the un-ionized cases): (A) conformation 1 and (B) conformation 2. These figures were created with RasMol.

group, the most hydrophobic portion of the dipeptide.

Results and Discussion

We analyzed the salt effects on the solubility of noble gases in water⁶ and the structure of pure water near a peptide and the solvation free energy.⁷ The information presented in refs. 6 and 7 is very useful to the present discussion. The solvation free energies are first discussed, and then they are related to the structure of the salt solution near the dipeptide.

SOLVATION FREE ENERGY

The solvation free energies calculated for case 1 are summarized in Table I. Those for the five

portions of the dipeptide [NH_2 , $\text{CHCH}_3(1)$, CONH , $\text{CHCH}_3(2)$, and COOH] are also given. The total solvation free energy (compare $\Delta\mu_s$ with $\Delta\mu_{s0}$) is increased by the salt addition in both of the two conformations (namely, the addition of salts makes the solute molecule less soluble). On the whole, I_C and I_A are negative and positive, respectively, and $|I_C| < |I_A|$ and $I_C + I_A > 0$. This result is consistent with that reported for noble gases⁶ (He, Ar, and Kr).

The solvation free energies calculated for case 2 are summarized in Table II with those for the five portions of the dipeptide. In pure water,⁷ water hydrogens are rather strongly bonded with the two carbonyl oxygens, 11 O Ala¹ and 21 O Ala² (i.e., the electrostatic bonds, 11 O Ala¹—H—O and 21 O Ala²—H—O, are formed). These electrostatic bonds in conformation 2 are stronger than those in conformation 1 due to the feature of conformation 2 mentioned in the last section.⁷ The total solvation free energy in conformation 2 is lower. These properties are also preserved in the 1 M NaCl solution. I_C and I_A for a portion with a positive (negative) net charge are positive (negative) and negative (positive), respectively, and their absolute values are very large. However, the sum of I_C and I_A is positive (with the exception that the sum is negative for CONH in conformation 1 and for CONH and COOH in conformation 2) and comparable with that in case 1. Again, the total solvation free energy is increased by the salt addition in both of the two conformations.

Here we comment on the convergence properties of the algorithm observed. We consider case 2 as an example. With the crude initial guess described above, convergence is achieved in 67 total outer-loop iterations for conformation 1. The time required for the construction and lower triangular–upper triangular (LU) decomposition¹ of the Jacobian matrix (the dimensionality of the matrix is 999) is ~ 2.6 min, and the time consumed for the rest of the calculation is ~ 4.6 min (i.e., the whole calculation is finished in ~ 7.2 min). Thus, the calculation of the solvation free energy for the dipeptide in the salt solution can be completed with minor computational effort on a workstation.

The solvation free energies calculated for case 3 are summarized in Table III. Those for the five portions of the dipeptide [NH_3^+ , $\text{CHCH}_3(1)$, CONH , $\text{CHCH}_3(2)$, and COO^-] are also given. In case 3 the dipeptide is ionized and present as a zwitterion. In pure water, the solvation free energy is much lower than that in the corresponding un-ionized case (compare Table III with

TABLE I.
Solvation Free Energies (SFE) Calculated for Case 1 (Un-ionized Dipeptide and All the Site Charges Set to 0)
and for Five Portions of Dipeptide.

Conf.	SFE	NH ₂	CHCH ₃ (1)	CONH	CHCH ₃ (2)	COOH	Total
1 ^a	$\Delta\mu_{S0}$	7.3	15.1	8.8	15.5	10.6	57.3
1 ^b	I_V	7.4	15.2	8.9	15.6	10.8	57.8
	I_C	-0.02	-0.08	-0.10	-0.08	-0.06	-0.34
	I_A	0.23	0.47	0.30	0.48	0.35	1.84
	$I_C + I_A$	0.21	0.39	0.20	0.40	0.29	1.50
	$\Delta\mu_S$	7.6	15.6	9.1	16.0	11.1	59.3
2 ^a	$\Delta\mu_{S0}$	7.4	13.9	9.0	16.9	8.8	56.0
2 ^b	I_V	7.4	14.0	9.2	17.0	8.9	56.5
	I_C	-0.02	-0.09	-0.10	-0.06	-0.07	-0.35
	I_A	0.24	0.43	0.30	0.53	0.29	1.80
	$I_C + I_A$	0.22	0.34	0.20	0.47	0.22	1.45
	$\Delta\mu_S$	7.5	15.5	9.0	16.0	10.9	57.9

Conformations 1 and 2 are considered. I_V , I_C , and I_A are interdependent but can be regarded as contributions of the structures of water molecules, cations, and anions near the dipeptide, respectively, and $\Delta\mu_S = I_V + I_C + I_A$. $\Delta\mu_{S0}$ denotes values for the dipeptide in pure water ($\Delta\mu_{S0} = I_V$). All the values are given in kilocalories/mole.

^a Pure water.
^b Salt solution (1 M NaCl).

Table II). That is, the zwitterion is more stable. The enhanced stability is dominated by the large negative contribution from the two oxygens in COO⁻. (The total charge is $-0.532e \times 2 = -1.064e$, where e is the electronic charge.) The contribution from the three hydrogens in NH₃⁺ is much smaller despite the fact that the magnitude of its total charge ($+0.285e \times 3 = +0.855e$) is considerably larger. There can be two major reasons for this. One is the

asymmetric (anisotropic) charge distribution in a water molecule in the sense that the two positive charges sit near the surface of the molecule whereas the negative charges rests at the center. As a result, an ionized group with a negative charge tends to form hydrogen bonding with water molecules more readily than that with a positive charge if the sizes and charge magnitudes of the groups are comparable.² The other is that the core sizes of the

TABLE II.
Solvation Free Energies (SFE) Calculated for Case 2 (Un-ionized Dipeptide and Full Values Assigned to Site Charges) and for Five Portions of Dipeptide.

Conf.	SFE	NH ₂	CHCH ₃ (1)	CONH	CHCH ₃ (2)	COOH	Total
1 ^a	$\Delta\mu_{S0}$	6.0	16.4	2.8	17.7	4.7	47.5
1 ^b	I_V	6.1	16.5	3.2	17.7	5.0	48.5
	I_C	-16.32	468.52	-469.11	468.59	-452.65	-0.97
	I_A	16.45	-468.19	469.07	-468.12	452.80	2.00
	$I_C + I_A$	0.13	0.33	-0.04	0.47	0.15	1.04
	$\Delta\mu_S$	6.2	16.8	3.2	18.2	5.2	49.6
2 ^a	$\Delta\mu_{S0}$	5.6	15.0	1.1	19.1	1.3	42.0
2 ^b	I_V	5.7	15.1	1.7	19.1	1.9	43.5
	I_C	-16.39	468.49	-469.16	468.63	-452.84	-1.28
	I_A	16.50	-468.24	468.97	-468.13	452.68	1.78
	$I_C + I_A$	0.11	0.25	-0.19	0.50	-0.16	0.50
	$\Delta\mu_S$	5.8	15.4	1.5	19.6	1.7	44.0

Conformations 1 and 2 are considered. I_V , I_C , and I_A are interdependent but can be regarded as contributions of the structures of water molecules, cations, and anions near the dipeptide, respectively, and $\Delta\mu_S = I_V + I_C + I_A$. $\Delta\mu_{S0}$ denotes values for the dipeptide in pure water ($\Delta\mu_{S0} = I_V$). All the values are given in kilocalories/mole.

^a Pure water.
^b Salt solution (1 M NaCl).

TABLE III.

Solvation Free Energies (SFE) Calculated for Case 3 (Dipeptide Is Present as Zwitterion and Full Values Assigned to Site Charges).

Conf.	SFE	NH ₃ ⁺	CHCH ₃ (1)	CONH	CHCH ₃ (2)	COO ⁻	Total
1 ^a	$\Delta\mu_{S0}$	0.7	17.4	1.3	18.2	-28.8	8.7
1 ^b	I_V	2.8	17.8	2.0	18.0	-25.0	15.5
	I_C	2051.65	468.49	-469.48	468.96	-2529.21	-9.59
	I_A	-2053.84	-468.40	469.15	-468.31	2525.93	4.53
	$I_C + I_A$	-2.2	0.09	-0.33	0.65	-3.28	-5.06
	$\Delta\mu_S$	0.6	17.9	1.6	18.7	-28.3	10.4
2 ^a	$\Delta\mu_{S0}$	2.1	16.1	-1.6	19.6	-36.2	-0.1
2 ^b	I_V	4.4	16.5	-0.5	19.4	-31.7	8.0
	I_C	2051.92	468.49	-469.87	469.03	-2529.66	-10.08
	I_A	-2054.09	-468.44	469.21	-468.29	2525.58	3.96
	$I_C + I_A$	-2.17	0.05	-0.66	0.74	-4.08	-6.12
	$\Delta\mu_S$	2.2	16.6	-1.2	20.1	-35.8	1.9

Conformations 1 and 2 are considered. I_V , I_C , and I_A are interdependent but can be regarded as contributions of the structures of water molecules, cation, and anions near the dipeptide, respectively, and $\Delta\mu_S = I_V + I_C + I_A$. $\Delta\mu_{S0}$ denotes values for the dipeptide in pure water ($\Delta\mu_{S0} = I_V$). All the values are given in kilocalories/mole.

^a Pure water.

^b Salt solution (1 M NaCl).

three hydrogens⁷ in NH₃⁺ (0.239 nm) are much larger than that of water hydrogens (0.040 nm). Effects due to the uncertainty of the σ values for the three hydrogens are to be investigated in further studies.

As observed in Table III, the degree of the decrease in the total solvation free energy caused by the ionization is larger in conformation 2 than in conformation 1, which is due to the feature of conformation 2 that the three oxygens are close together. This is true both in pure water and in the 1 M NaCl solution. Unlike in cases 1 and 2, $I_C + I_A$ for NH₃⁺ and COO⁻ have relatively large, negative values. However, I_V in the solution is considerably larger than that in pure water. As a result, for these two portions $\Delta\mu_S$ do not differ significantly from $\Delta\mu_{S0}$. The total solvation free energy is again increased by the salt addition in both of the two conformations.

It is interesting to note that I_C (total) and I_A (total) are always negative and positive, respectively, for both of the two conformations and in all the three cases. The I_V in the salt solution is always larger than that in pure water, and this is particularly true in case 3. The sum, $I_C + I_A$ (total), is positive in cases 1 and 2 and negative in case 3.

STRUCTURE OF SALT SOLUTION

The site-site pair distribution functions $g_{ab}(r)$ for $a = 1$ H Ala¹ and $a = 22$ O Ala² are shown in Figures 2 and 3, respectively. In cases 1 and 2 the

1 H Ala¹ is one of the two hydrogens in NH₂, and in case 3 it is one of the three hydrogens in NH₃⁺. In cases 1 and 2 the 22 O Ala² is the hydroxyl oxygen in COOH, and in case 3 it is one of the two oxygens in COO⁻. In case 1, as observed in Figures 2(a) and 3(a), $r_{\max, aC} > r_{\max, aA}$ [$r_{\max, ab}$ denotes the first-peak position of $g_{ab}(r)$] despite the fact that $\sigma_C < \sigma_A$. In other words, cations stay less close to atoms of the solute molecule than anions. This is ascribed to the specific orientational order of water molecules near the atoms.⁶ For cations, $r_{\max, aC}$ is considerably larger than σ_{aC} (i.e., $r_{\max, aC}$ is in the region where u_{aC} is weakly attractive), whereas for anions $r_{\max, aA} \sim \sigma_{aA}$ and g_{aA} is significantly large even in the region where u_{aA} is considerably repulsive. As a consequence, I_C and I_A are negative and positive, respectively, and $|I_C| < |I_A|$. It is interesting to note that the qualitative aspects of the conclusions drawn for noble gases⁶ are also applicable to a hydrophobic molecular solute.

In case 2 electrostatic bonds are formed between 1 H Ala¹ and anions (Cl⁻), 22 O Ala² and cations (Na⁺), and 22 O Ala² and water hydrogens [see Figs. 2(b), 3(b)]. These bounds are considerably enhanced in case 3 [compare Fig. 2(b) with 2(c) and Fig. 3(b) with 3(c)], and bond formation between 1 H Ala¹ and water oxygens also becomes significant. In particular, the first-peak values of $g_{ab}(r)$ for $a = 22$ O Ala² and $b = \text{H}$ and C are greatly increased by the ionization. There are two reasons for this⁷: 22 O Ala² is covalently bonded with one carbon alone in case 3 while it is with one

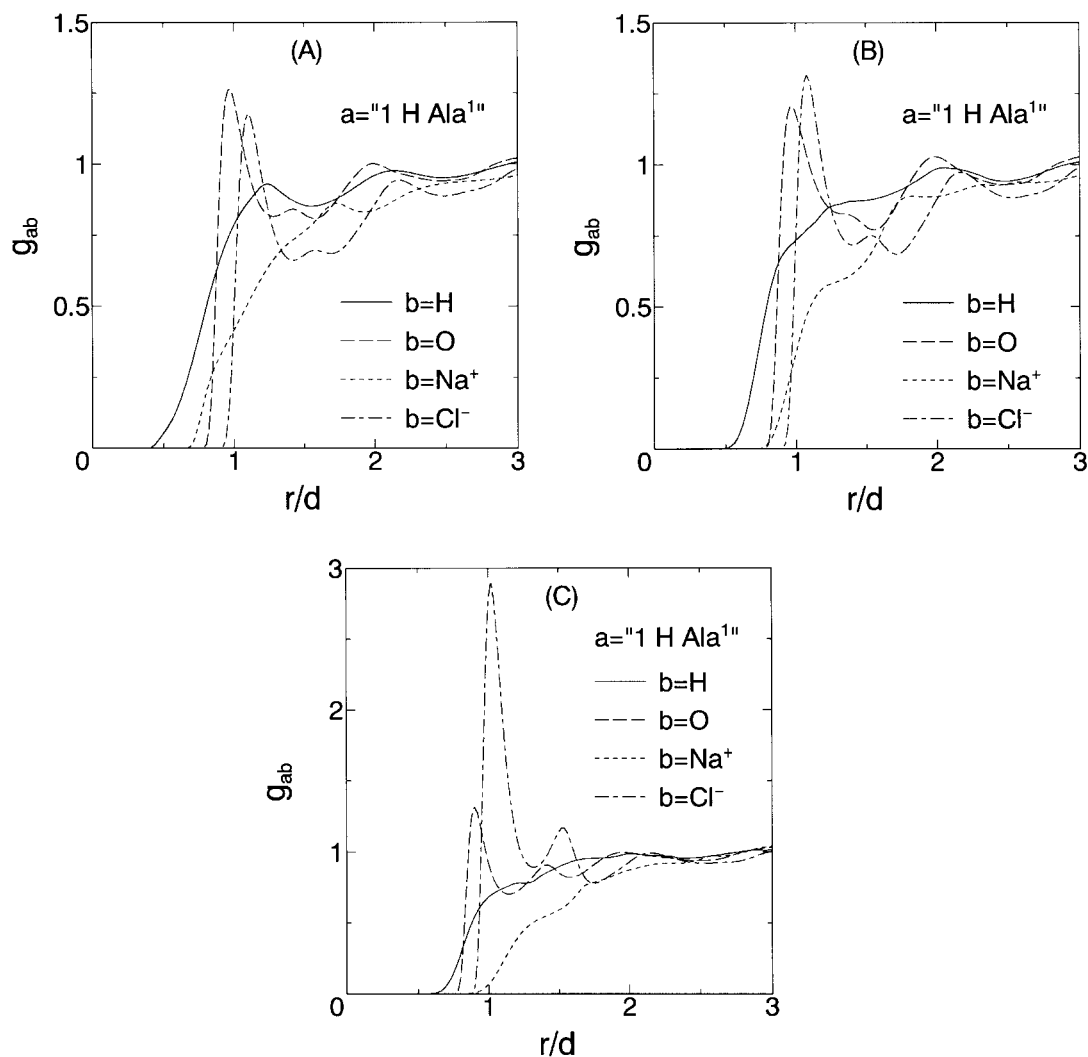


FIGURE 2. Site-site pair distribution functions $g_{ab}(r)$ of the dipeptide in conformation 1 ($d = 0.28$ nm): $a = 1 \text{ H Ala}^1$ and $b =$ water hydrogens (H), water oxygens (O), cations (Na^+), and anions (Cl^-). (A) Case 1 where the dipeptide is un-ionized and all the site charges are set to zero. (B) Case 2 where the dipeptide is un-ionized and the full values are assigned to the site charges. (C) Case 3 where the dipeptide is present as a zwitterion and the full values are assigned to the site charges. In cases 1 and 2 the 1 H Ala^1 is one of the two hydrogens in NH_2 , and in case 3 it is one of the three hydrogens in NH_3^+ .

carbon and one hydrogen in case 2; and the magnitude of the site charge of 22 O Ala^2 in case 3 ($-0.532e$) is larger than that in case 2 ($-0.380e$).

In case 3 anions and cations form strong electrostatic bonds with the three hydrogens in NH_3^+ and with the two oxygens in COO^- , respectively. This is particularly true for cations and the two oxygens. The I_A for NH_3^+ and I_C for COO^- become very large, negative values and $I_C + I_A$ for these two portions are also negative. However, the electrostatic bonds, water oxygens—the three hydrogens in NH_3^+ and water hydrogens—the two oxy-

gens in COO^- , are somewhat disturbed with the result of the significant increase in I_V .

The difference, $\Delta\mu_S - \Delta\mu_{S0}$, remains almost unchanged for both of the two conformations and in all the three cases tested (for conformation 1, the values are 2.0, 2.1, and 1.7 kcal/mol in cases 1, 2, and 3, respectively; for conformation 2, the values are 1.9, 2.0, and 2.0 kcal/mol in cases 1, 2, and 3, respectively). In determination of the most stable conformation of a peptide in salt solutions, the sum of the conformational energy and the solvation free energy⁷ is a criterion function to be mini-

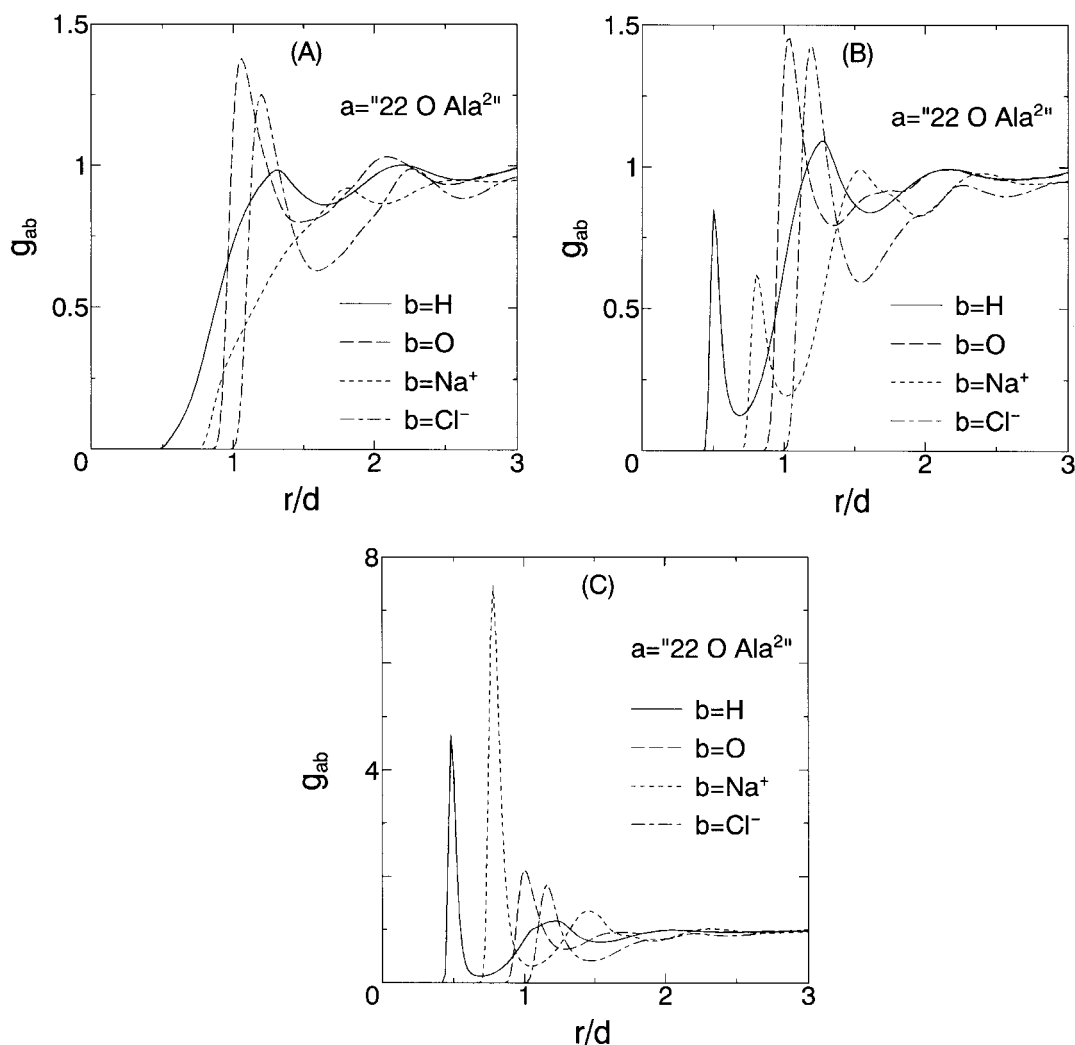


FIGURE 3. Site-site pair distribution functions $g_{ab}(r)$ of the dipeptide in conformation 1 ($d = 0.28$ nm): $a = 22$ O Ala²⁺ and $b =$ water hydrogens (H), water oxygens (O), cations (Na⁺), and anions (Cl⁻). (A) Case 1 where the dipeptide is un-ionized and all the site charges are set to zero. (B) Case 2 where the dipeptide is un-ionized and the full values are assigned to the site charges. (C) Case 3 where the dipeptide is present as a zwitterion and the full values are assigned to the site charges. In cases 1 and 2 the 22 O Ala²⁺ is the hydroxyl oxygen in COOH, and in case 3 it is one of the two oxygens in COO⁻.

mized. However, our result suggests that for a very small peptide the conformational stability could be analyzed by replacing the salt solution by pure water, as long as the salt concentration is sufficiently low (lower than ~ 1 M). However, for larger peptides with ionized residues (e.g., His⁺ and Glu⁻) that can be close together, the presence of salts can affect the conformational stability to a large extent, which must be investigated in further studies.

We found that the site-site pair distribution functions $g_{ab}(r)$ for $b = C$ and A (especially the first-peak values) are somewhat sensitive to the solute-ion potential parameters. Pettitt et al.^{23,24}

and Marlow et al.^{24,25} studied 1 M NaCl and 1 M CH₃COONa solutions near the zwitterionic bis(penicillamine) enkephalin derivative (DPDPE) using the molecular dynamics simulation. According to their results, sodium-ion binding to the backbone carbonyl groups near the negatively charged C terminus occurs in the 1 M CH₃COONa solution, which is in qualitative accord with our result. In their result for 1 M NaCl solution, however, sodium ions did not associate directly with the peptide. In both of the solutions, anions (particularly Cl⁻) associated closely with the N terminus and amide hydrogens of the peptide. In our case, anions associate only with the N terminus

hydrogens. It may be interesting to consider the DPDPE in the 1M NaCl solution with the RISM theory by employing the same models for the DPDPE, water molecules, cations, and anions (i.e., the same potential-energy functions and parameters) and to compare the result with the simulation results. Work in this direction is planned. We note that the qualitative aspects of our conclusions on the solvation free energies are not significantly affected by the uncertainty of the solute-ion potential parameters.

COMPARISON WITH OTHER RISM RESULTS

It is now obvious that our result conflicts with the result reported by Perkyns and colleagues.^{8,9} They treated a zwitterionic tripeptide of sequence Gly-Ala-Gly in high concentration NaCl solution. Many conformations of the peptide were tested, and below 3 M stable solutions of the RISM-HNC theory could never be found with the Picard method. In contrast, we readily found stable solutions for our peptide in the 1 M NaCl solution. We tested conformation 1 in case 3 with the salt concentration of 0.5 M: the convergence was achieved with no difficulty (total solvation free energy = 9.7 kcal/mol). Moreover, the results of Perkyns and colleagues indicates that the peptide is salted into solution by the cosolvent NaCl, which contradicts with our result and the general observation that NaCl often salts many peptides out of solution.

It is not definite if the results of Perkyns et al.^{8,9} was due to numerical instability of the Picard method or physical instability. In the Picard method the Jacobian matrix is simply set to the identity matrix.²⁶ For strongly coupled fluid particles the correct matrix is far from the identity matrix, and the Picard method often becomes useless. We emphasize that there are many examples (e.g., molten salts^{26,27}, both the metal^{28,29} and the fluid²⁹⁻³¹ calculations for aqueous electrolytes near metal walls, some peptides in pure water or salt solution,^{1,5} inhomogeneous fluids confined between two walls,³² etc.) where severe instability was caused by the Picard method whereas convergence was readily achieved with the hybrid method. Of course, it is possible that Perkyns et al. encountered physical instability: the behavior of a peptide-salt solution system can be strongly dependent on the peptide species and model potential energy functions and parameters used. In fact, while many peptides are salted out of solution by NaCl, there are exceptions like β -lactoglobulin⁹

that are salted in by NaCl. Further studies are needed to clarify these points.

Conclusion

We developed an algorithm for solving the RISM equations for salt solutions near a solute molecule with many atomic sites. It was obtained as an extension of our previously reported algorithm for pure water near the solute molecule. The great advantages of the algorithm for the pure water case¹ (e.g., the constant Jacobian matrix) were all preserved. We emphasize that no approximate treatment was employed to accelerate the calculation. The robustness and high efficiency of the algorithm was demonstrated for a dipeptide ($\text{NH}_2\text{—CHCH}_3\text{—CONH—CHCH}_3\text{—COOH}$; Ala-Ala) with two conformations in a 1 M NaCl solution. The SPC/E model was chosen for water molecules.

Three different cases were considered. In cases 1 and 2 the dipeptide was un-ionized, but in case 3 it was ionized and present as a zwitterion. In case 1 all the site charges of the dipeptide were set to zero, but in cases 2 and 3 the full values were assigned to the site charges. The qualitative aspects of the solvation structure observed in case 1 were similar to those previously obtained for noble gases in salt solutions. For example, cations stayed less closer to atoms of the dipeptide; contributions of cations and anions to the solvation free energy (I_C and I_A) were negative and positive, respectively; and $|I_C| < |I_A|$.

In case 2 electrostatic bonds were formed between 1 H Ala¹ and anions (Cl^-), 22 O Ala² and cations (Na^+), and 22 O Ala² and water hydrogens, for example. These bonds were considerably enhanced in case 3, and bond formation between 1 H Ala¹ and water oxygens also became significant. In case 3 anions and cations formed strong electrostatic bonds with the three hydrogens in NH_3^+ and with the two oxygens in COO^- , respectively, and I_A for NH_3^+ and I_C for COO^- became very large, negative values. The sum $I_A + I_C$ for these two portions was also negative. However, the electrostatic bonds, water oxygens—the three hydrogens in NH_3^+ and water hydrogens—the two oxygens in COO^- , were somewhat disturbed by those ions with the result of the significant increase in I_V (contribution of water molecules to the solvation free energy).

The I_C (total) and I_A (total) were always negative and positive, respectively, for both of the two

conformations and in all the three cases considered. The sum $I_C + I_A$ (total) was positive in cases 1 and 2 and negative in case 3. The I_V in the salt solution was always larger than that in pure water, and this was particularly true in case 3. The total solvation free energy was always increased (i.e., the dipeptide became less soluble) by the salt addition. Moreover, the increase $\Delta\mu_S - \Delta\mu_{S0}$ remained almost constant (~ 2 kcal/mol) against conformational changes and the ionization.

Next, we comment on the computer storage requirements and the computation time of our algorithm. In the pure water case, the storage requirements for the Jacobian matrix were less than those for the intramolecular correlations of the solute molecule; but this was not true in the salt-solution case. When a very large solute is treated, the size of the Jacobian matrix will become extremely large and a very long computer time will be required to generate it. We believe, however, that even such a problem can be overcome by modifying the construction of the hybrid algorithm: there is no need to apply the Newton–Raphson method to all the solute–water and –ion correlations (details will be described in a future article). Or if necessary, we might consider some techniques^{33,34} of avoiding direct manipulation of the huge matrix (in fact, there is no need to actually generate it and store it), although the robustness and efficiency will be somewhat deteriorated (but still, the resultant algorithm is far superior to the Picard method).

Perkyns et al.^{8,9} solved the full RISM equations for a model of a zwitterionic tripeptide of sequence Gly-Ala-Gly in high concentration NaCl solution. The Picard method was employed in their work. Their result conflicts with ours in the following two respects: they claim that the RISM-HNC theory possesses no solutions for the system below 3 M; and the peptide is salted into solution by NaCl. It is possible that the behavior of a peptide–salt solution system is strongly dependent on the peptide species and model potential-energy functions and parameters used. The reasons for this conflict must be clarified in future studies. We also plan to study effects due to the salt species (e.g., LiCl, NaCl, KCl, KBr, KI, etc.). Larger peptides (including those with ionized residues such as His⁺ and Glu[−] which can get close together) will also be considered. Our algorithm and/or its modified versions will be very useful in these future studies.

References

1. M. Kinoshita, Y. Okamoto, and F. Hirata, *J. Comput. Chem.*, **18**, 1320 (1997).
2. H. J. C. Berendsen, J. R. Grigera, and T. P. Straatsma, *J. Phys. Chem.*, **91**, 6269 (1987).
3. B. M. Pettitt and M. Karplus, *Chem. Phys. Lett.*, **121**, 194 (1985).
4. G. L. Ramé, W. F. Lau, and B. M. Pettitt, *Int. J. Peptide Protein Res.*, **35**, 315 (1990).
5. F. Hirata and M. Kinoshita, unpublished results.
6. M. Kinoshita and F. Hirata, *J. Chem. Phys.*, **106**, 5202 (1997).
7. M. Kinoshita, Y. Okamoto, and F. Hirata, *J. Chem. Phys.*, **107**, 1586 (1997).
8. J. S. Perkyns and B. M. Pettitt, *J. Phys. Chem.*, **99**, 1 (1995).
9. J. S. Perkyns, Y. Wang, and B. M. Pettitt, *J. Am. Chem. Soc.*, **118**, 1164 (1996).
10. J. S. Perkyns and B. M. Pettitt, *Chem. Phys. Lett.*, **190**, 626 (1992).
11. J. S. Perkyns and B. M. Pettitt, *J. Chem. Phys.*, **97**, 7656 (1992).
12. D. A. Zichi and P. J. Rossky, *J. Chem. Phys.*, **84**, 1712 (1986).
13. H. A. Yu, B. Roux, and M. Karplus, *J. Chem. Phys.*, **92**, 5020 (1990).
14. M. Kinoshita and D. R. Bérard, *J. Comput. Phys.*, **124**, 230 (1996).
15. M. Kinoshita and F. Hirata, *J. Chem. Phys.*, **104**, 8807 (1996).
16. H. Kawai, Y. Okamoto, M. Fukugita, T. Nakazawa, and T. Kikuchi, *Chem. Lett.*, **1991**, 213 (1991); Y. Okamoto, M. Fukugita, T. Nakazawa, and H. Kawai, *Protein Eng.*, **4**, 639 (1991).
17. F. A. Momany, R. F. McGuire, A. W. Burgess, and H. A. Scheraga, *J. Phys. Chem.*, **79**, 2361 (1975).
18. G. Némethy, M. S. Pottle, and H. A. Scheraga, *J. Phys. Chem.*, **87**, 1883 (1983).
19. M. J. Sippl, G. Némethy, and H. A. Scheraga, *J. Phys. Chem.*, **88**, 6231 (1984).
20. B. M. Pettitt and P. J. Rossky, *J. Chem. Phys.*, **84**, 5836 (1986).
21. C. Mavroyannis and M. J. Stephen, *Mol. Phys.*, **5**, 629 (1962).
22. F. Hirata, P. Redfen, and R. M. Levy, *Int. J. Quantum Chem.*, **15**, 179 (1988).
23. P. E. Smith and B. M. Pettitt, *J. Am. Chem. Soc.*, **113**, 6029 (1991).
24. G. E. Marlow, J. S. Perkyns, and B. M. Pettitt, *Chem. Rev.*, **93**, 2503 (1993).
25. P. E. Smith, G. E. Marlow, and B. M. Pettitt, *J. Am. Chem. Soc.*, **115**, 7493 (1993).
26. M. Kinoshita and M. Harada, *Mol. Phys.*, **65**, 599 (1988).
27. G. M. Abernethy and M. J. Gillan, *Mol. Phys.*, **39**, 839 (1980).
28. P. Gies and R. R. Gerhardts, *Phys. Rev. B*, **33**, 982 (1986).
29. D. R. Bérard, M. Kinoshita, X. Ye, and G. N. Patey, *J. Chem. Phys.*, **101**, 6271 (1974).
30. D. R. Bérard, M. Kinoshita, X. Ye, and G. N. Patey, *J. Chem. Phys.*, **102**, 1024 (1995).
31. D. R. Bérard, M. Kinoshita, N. M. Cann, and G. N. Patey, *J. Chem. Phys.*, **107**, 4719 (1997).
32. F. Otto and G. N. Patey, private communication.
33. G. Zerah, *J. Comput. Phys.*, **61**, 280 (1985).
34. A. Busigin and C. R. Phillips, *Mol. Phys.*, **76**, 89 (1992).